ISSN 1070-3284, Russian Journal of Coordination Chemistry, 2023, Vol. 49, No. 11, pp. 718–729. © Pleiades Publishing, Ltd., 2023.
Russian Text © The Author(s), 2023, published in Koordinatsionnaya Khimiya, 2023, Vol. 49, No. 11, pp. 693–705.

Coordination Polymer or Cluster: Zinc Bis(3,5-di-*tert*-octyl-semiquinolate) with Pyrazine

A. V. Maleeva[a], *, O. Yu. Trofimova[a], T. N. Kocherova[a], I. A. Yakushev[b], A. S. Bogomyakov[c], and A. V. Piskunov[a], **

[a] *Razuvaev Institute of Organometallic Chemistry, Russian Academy of Sciences, Nizhny Novgorod, Russia*
[b] *Kurnakov Institute of General and Inorganic Chemistry, Russian Academy of Sciences, Moscow, Russia*
[c] *International Tomography Center, Siberian Branch, Russian Academy of Sciences, Novosibirsk, Russia*
**e-mail: arina@iomc.ras.ru*
***e-mail: pial@iomc.ras.ru*

Received April 10, 2023; revised May 11, 2023; accepted May 15, 2023

Abstract—New zinc bis-*o*-semiquinolate complexes based on 3,5-di-*tert*-octyl-*o*-benzoquinone bearing the N-donor ligand (pyrazine) coordinated to the metal are synthesized. Two different products can be obtained depending on the synthesis method: coordination polymer (direct oxidation of metallic zinc with *o*-quinone (CIF file CCDC no. 2250574 (**I**)) or polynuclear cluster (exchange reaction (CIF file CCDC no. 2250575 (**II**)). The coordination polymer is linear and free of intermolecular π,π interactions between the aromatic fragments of the adjacent molecules. The magnetochemical study of complexes **I** and **II** shows that intramolecular antiferromagnetic exchange interactions between spins of the *o*-semiquinolate radical centers dominate.

Keywords: redox-active ligand, *o*-quinones, coordination polymers, zinc, XRD, magnetic susceptibility
DOI: 10.1134/S1070328423600742

INTRODUCTION

Interest in the *o*-quinone [1–3] (and related *o*-iminoquinone [2, 4–8]) complexes of the predominant majority of the known metals appeared more than fifty years ago and nowadays remains at the same level. This is not surprising because numerous interesting phenomena, such as valence tautomerism [5, 9–16], photo- and thermal sensitivity of a series of molecular crystals [17–19], fixation of small molecules [20, 21]), including reversible fixation [21], selective catalysis [22], activating complexation [23, 24], intramolecular interligand charge transfer in chromophoric systems based on the *o*-quinone coordination metal complexes [25–32] capable of generating photoinduced high-spin molecules [33–40], and others, have been discovered to the present time. Note that some aforementioned discoveries are valid for the nontransition metal derivatives in spite of the quite justified popularity of the transition metal compounds in the presented studies [20–22].

Polyradical metal complexes with redox-active ligands are also of interest as possible building blocks for the preparation of molecular magnets [41–47]. *o*-Quinone and iminoquinone complexes of transition metals in which two and more organic ligands exist in the stable anion-radical form were studied in rather detail and are characterized by superexchange channels associated with a significant involvement of the paramagnetic ion of the complexing agent in the exchange processes [1, 5, 48–50]. However, the study of simpler systems seems fairly urgent for a deeper understanding of intramolecular interligand exchange processes. Polyspin *o*-quinone derivatives of nontransition metals are especially suitable for the solution of similar problems. A series of our recent work was focused on establishing magnetostructural relationships for the *o*-quinone complexes of Group II metals [51–53]. The zinc, magnesium, and cadmium compounds with the penta- and hexacoordinate environment of the metallocenter were studied. Summarizing the aforementioned data, we can say that the compounds with the square pyramidal environment are characterized by stronger intramolecular exchanges, and the octahedral geometry demonstrates more modern values of the interaction between spins of the adjacent ligands. An inversely proportional relationship of the distance between radical centers in the zinc complexes and the exchange interaction was revealed for a series of the complexes of the same type [52, 53]. The antiferromagnetic intramolecular exchange between radical centers of the adjacent ligand is characteristic of the most type of the synthesized zinc, magnesium, and cadmium *o*-semiquinolate derivatives [52–54]. Among a few exceptions is the series of

zinc bis-*o*-semiquinolates with the bidentate N,N-donor ligands (2,2'-bipyridyl, phenanthroline, and 2,9-dimethyl-1,10-phenanthroline) [51] demonstrating the unusual (for similar systems) ferromagnetic interaction between unpaired electrons of adjacent ligands. However, in all complexes studied by us, the absolute value of exchange parameters turned out to slightly differ from zero regardless of the geometric features of the coordination nodes. This is due to numerous intermolecular exchanges comparable in value and most frequently inverse in sign to intramolecular exchanges. Negligible total magnetic effects are a consequence of similar disguise [51, 53, 55].

A similar intermolecular effect of adjacent molecules can be excluded and true intramolecular exchanges can be observed due to the real spatial separation of adjacent molecules at distances that do not allow intermolecular ligand exchange channels to appear as it took place in magnesium bis-*o*-semiquinolate with the iminopyridine ligand [53]. A similar concept can also be accomplished by using *o*-quinone ligands with strong steric hindrance such as *o*-quinone with *tert*-octyl substituents.

The task on the synthesis of zinc bis-*o*-semiquinolate based on 3,5-di-*tert*-octyl-*o*-benzoquinone with pyrazine and the study of its magnetic behavior was stated in the framework of the above concept.

EXPERIMENTAL

All procedures on the synthesis and study of chemical transformations of the zinc complexes were carried out without air oxygen and moisture access. The solvents used were purified and dehydrated according to published recommendations [56]. Commercially available metallic Zn, pyrazine, and crystalline I_2 (all Aldrich) were used. 3,5-Di-*tert*-octyl-*o*-benzoquinone was synthesized using a known procedure [57]. IR spectra were recorded on an FSM-1201 FT-IR spectrometer (suspensions in Nujol, KBr cells). Elemental analysis was conducted on an Elementar Vario El cube instrument. The magnetic susceptibility of the polycrystalline complexes was measured on a Quantum Design MPMSXL SQUID magnetometer in the 2–300 K temperature range in a magnetic field of 0.5 T.

Synthesis of $((3,5\text{-}^t\text{Oc-SQ})_2\text{Zn}\cdot(\text{Pyr})\cdot 3C_5H_{12})_n$ (I). Zinc bis-*o*-semiquinolate based on 3,5-di-*tert*-octyl-*o*-benzoquinone (3,5-^{t}Oc-Q) was synthesized by analogy to the known procedure for the synthesis of zinc 3,6-di-*tert*-butyl-bis-*o*-semiquinolate [58]. A solution of 3,5-^{t}Oc-Q (0.66 g, 2 mmol) in tetrahydrofuran (THF) on heating was subjected to the reaction with amalgamated zinc, and the mixture was stirred for 2 h until the reaction mixture became completely colorless. The formed solution was filtered from the amalgam on the Schott filter no. 4, and an equivalent amount of 3,5-^{t}Oc-Q (0.66 g, 2 mmol) was added to form a bright blue solution. A solution of pyrazine (0.16 g, 2 mmol) in THF was added to the resulting solution. The liquid phase was evaporated under reduced pressure, and the residue was dissolved in pentane. The obtained solution was stored at −10°C to form dark blue finely crystalline product **I**. The yield of complex **I** was 1.82 g (89%).

For $C_{48}H_{76}N_2O_4Zn\cdot 3C_5H_{12}$			
Anal. calcd., %	C, 73.68	H, 10.99	N, 2.73
Found, %	C, 73.38	H, 10.94	N, 2.72

IR (ν, cm^{-1}): 1747 m, 1665 m, 1584 s, 1519 s, 1485 s, 1418 s, 1395 s, 1362 s, 1345 s, 1319 m, 1287 m, 1239 s, 1213 s, 1156 m, 1132 m, 1086 m, 1075 m, 1043 s, 1028 w, 1016 m, 1010 m, 993 s, 974 m, 943 w, 922 m, 886 w, 868 s, 853 m, 826 m, 803 m, 791 m, 770 m, 750 w, 739 w, 700 w, 679 m, 622 m, 576 m, 546 m, 533 w, 518 w, 500 m.

Synthesis of $((3,5\text{-}^t\text{Oc-SQ})_2\text{ZnINa(Pyr)(THF)})_2$ (II) was carried out similarly to a published procedure [59]. A solution of zinc diiodide (0.64 g, 2 mmol) was prepared by mixing a solution of iodine in THF on heating above zinc amalgam until the iodine color disappeared completely followed by decanting from the metal. A solution of 3,5-^{t}Oc-SQNa (1.42 g, 4 mmol) in THF was poured to a solution of zinc diiodide in the same solvent. Then THF was removed under reduced pressure, and the residue was dissolved in toluene and subjected to the interaction with a solution of pyrazine (0.16 g, 2 mmol) in the same solvent. The subsequent replacement of toluene by hexane made it possible to obtain blue finely crystalline product **II**. The yield of complex **II** was 1.96 g (94%).

For $C_{104}H_{168}N_4O_{10}I_2Na_2Zn_2$			
Anal. calcd., %	C, 60.49	H, 8.20	N, 2.71
Found, %	C, 60.26	H, 8.24	N, 2.70

IR (ν, cm^{-1}): 1623 w, 1608 w, 1582 s, 1518 s, 1484 s, 1455 s, 1412 s, 1393 s, 1362 s, 1343 m, 1320 m, 1286 m, 1238 s, 1213 m, 1182 w, 1148 m, 1130 w, 1121 w, 1082 m, 1065 m, 1056 m, 1026 s, 1008 m, 993 s, 975 m, 943 w, 922 m, 900 w, 887 w, 870 m, 862 m, 853 m, 826 m, 811 m, 794 s, 770 m, 740 w, 680 m, 671 m, 576 m, 549 s, 533 w, 508 m, 500 m.

XRD of single crystals of compounds **I** and **II** were carried out on a Bruker D8 Venture Photon X-ray diffractometer (MoK_α, λ = 0.71073 Å, φ and ω scan modes, Incoatec IμS 3.0 microfocus X-ray radiation source) at 150 (for **I**) and 100 K (for **II**) at the Center for Collective Use of Physical Methods of Investigation at the Kurnakov Institute of General and Inorganic Chemistry (Russian Academy of Sciences). The primary indexing and refinement of unit cell parameters and integration of experimental reflection intensities were performed using the Bruker APEX3 software

Table 1. Crystallographic data and selected structure refinement parameters for complexes **I** and **II**

Parameter	Value	
	I	**II**
Composition	$C_{48}H_{76}N_2O_4Zn \cdot 3C_5H_{12}$	$C_{104}H_{168}N_4O_{10}I_2Na_2Zn_2$
FW	810.47	2064.93
Crystal system	Orthorhombic	Tetragonal
Space group	*Ccca*	$I4_1/a$
a, Å	23.5481(14)	35.682(2)
b, Å	30.2146(18)	35.682(2)
c, Å	14.8464(9)	17.0518(10)
α, deg	90	90
β, deg	90	90
γ, deg	90	90
V, Å^3	10563.2(11)	21710(3)
Z	8	8
ρ_{calc}, g/cm^3	1.019	1.264
μ, mm^{-1}	0.502	1.073
Crystal sizes, mm	0.090 × 0.070 × 0.070	0.090 × 0.060 × 0.020
Scan range over θ, deg	2.193–30.564	2.088–25.057
Number of measured/independent reflections	78005/8096	63230/9604
R_{int}	0.0591	0.0614
Number of reflections with $I > 2\sigma(I)$	8096	9604
Number of refined parameters/restraints	260/0	674/351
R ($F^2 > 2\sigma(F^2)$)	$R_1 = 0.0439$, $wR_2 = 0.1125$	$R_1 = 0.0484$, $wR_2 = 0.1088$
R (for all data)	$R_1 = 0.0722$, $wR_2 = 0.1254$	$R_1 = 0.0714$, $wR_2 = 0.1168$
S (F^2)	1.033	1.059
Residual electron density (max/min), e/Å^3	0.684/–0.496	0.646/–0.692

[60]. Absorption corrections of reflection intensities were applied using the SADABS program [61]. The structures of complexes **I** and **II** were solved by direct methods [62] and refined by full-matrix least squares for F^2 [63] in the anisotropic approximation for all non-hydrogen atoms without any restraints to thermal or geometric parameters of the structure in the case of complex **I**. In the case of complex **II**, the disordered carbon atoms of the *tert*-butyl groups, carbon and oxygen atoms of the coordinated THF molecules, and nitrogen and carbon atoms of partially disordered pyrazine were refined using the corresponding restraints to the geometric (SADI, FLAT instructions) and thermal (SIMU, RIGU instructions) parameters of the model. The residual electron density in the structure of complex **I** assigned to the solvate disordered over numerous positions solvent was removed from the model using the SQUEEZE procedure [64]. Hydrogen atoms were placed in the calculated positions and refined in the riding model with $U_{iso}(H) = 1.5U_{eq}(C)$ for the hydrogen atoms of the methyl groups and $1.2U_{eq}(O)$ for all other hydrogen atoms. The calculations were performed using the SHELXTL software [62, 63] in the OLEX2 medium of structural data processing and visualization [65]. The crystallographic data and XRD experimental and structure refinement parameters are given in Table 1. Selected bond lengths and angles are given in Table 2.

The full sets of XRD parameters for compounds **I** and **II** were deposited with the Cambridge Crystallographic Data Centre (CIF files CCDC nos. 2250574 (**I**) and 2250575 (**II**); ccdc.cam.ac.uk/structures).

RESULTS AND DISCUSSION

By analogy to the earlier studies of the biradical derivatives of Group II metals based on 3,6-di-*tert*-

Table 2. Selected bond lengths (Å) and angles (deg) for complexes **I** and **II***

Bond	**I**	**II**
	d, Å	
Zn(1)–O(1)	2.0271(11)	2.015(3)
Zn(1)–O(2)	2.0425(11)	2.079(3)
Zn(1)–O(3)		2.040(3)
Zn(1)–O(4)		2.082(3)
Zn(1)–I(1)		2.5836(6)
Zn(1)–N(1)	2.234(2)	
Zn(1)–N(2)	2.396(2)	
Na(1)–O(2)		2.320(3)
Na(1)–O(4)		2.406(3)
Na(1)–O(5)		2.42(2)
Na(1)–I(1)		3.1960(15)
Na(1)–N(1)		2.630(5)
Na(1)–O(4A)		2.503(3)
O(1)–C(1)	1.2850(18)	1.262(5)
O(2)–C(2)	1.2791(19)	1.277(5)
C(1)–C(2)	1.472(2)	1.467(5)
C(2)–C(3)	1.441(2)	1.406(6)
C(3)–C(4)	1.375(2)	1.361(6)
C(4)–C(5)	1.431(2)	1.436(6)
C(5)–C(6)	1.370(2)	1.354(6)
C(1)–C(6)	1.413(2)	1.447(6)
C(7)–C(8)		1.465(5)
C(8)–C(9)		1.403(5)
C(9)–C(10)		1.361(5)
C(10)–C(11)		1.437(5)
C(11)–C(12)		1.364(6)
C(12)–C(7)		1.434(5)
Angle	ω, deg	
O(1)Zn(1)O(2)	81.80(4)	79.92(10)
O(1)Zn(1)O(2A)	98.07(4)	

Table 2. (Contd.)

Angle	I	II
	ω, deg	
O(1)Zn(1)O(1A)	178.14(6)	
O(1)Zn(1)N(1)	90.93(3)	
O(1)Zn(1)N(2)	89.07(3)	
O(1)Zn(1)O(3)		91.54(11)
O(1)Zn(1)O(4)		143.07(11)
O(1)Zn(1)I(1)		110.72(8)
O(2)Zn(1)O(3)		139.55(11)
O(2)Zn(1)O(4)		84.16(10)
O(2)Zn(1)I(1)		111.76(8)
O(2)Zn(1)O(2A)	172.31(6)	
O(2)Zn(1)O(1A)	89.07(3)	
O(2)Zn(1)N(1)	93.85(3)	
O(2)Zn(1)N(2)	86.15(3)	
N(1)Zn(1)N(2)	180.0	
O(3)Zn(1)O(4)		79.41(10)
O(3)Zn(1)I(1)		108.26(8)
O(2)Na(1)O(4)		72.31(10)
O(2)Na(1)O(5)		90.8(4)
O(2)Na(1)N(1)		101.00(13)
O(2)Na(1)I(1)		174.27(10)
O(2)Na(1)O(4A)		97.75(10)
O(4)Na(1)O(5)		96.6(6)
O(4A)Na(1)N(1)		96.6(6)
O(4)Na(1)I(1)		102.00(8)
O(4)Na(1)O(4A)		74.58(10)
O(4A)Na(1)O(5)		165.0(6)
O(4A)Na(1)I(1)		81.07(7)
O(4)Na(1)N(1)		168.03(14)
N(1)Na(1)I(1)		84.72(10)
O(5)Na(1)I(1)		91.1(2)
O(5)Na(1)N(1)		93.4(6)
O(2)Na(1)O(4A)		97.75(10)
Zn(1)I(1)Na(1)		73.68(3)
Zn(1)O(4)Na(1)		99.09(11)

* Symmetry transforms used for the generation of equivalent atoms: (A) $-x + 3/2, -y + 1, z$; (B) $x, -y + 1, z + 1/2$; (C) $x, -y + 1, z - 1/2$ (**I**). (A) $-x + 1/2, -y + 1/2, -z + 3/2$ (**II**).

butyl-*o*-benzoquinone [58], the zinc bis-*o*-semiquinolate complex ((3,5-^{t}Oc-SQ)$_2$Zn(THF)$_2$) based on 3,5-di-*tert*-octyl-*o*-benzoquinone was synthesized via Scheme 1. The synthesized zinc bis-3,5-di-*tert*-octyl-*o*-semiquinolate was subjected in situ to the reaction with pyrazine in a ratio of 1 : 1 to form a bright blue solution of metal-organic framework (MOF) **I** (Scheme 1). The crystals of polymer complex **I** suitable for XRD were isolated upon a prolong storage of the reaction system in pentane at −10°C. The molecular and crystal structures of complex **I** were determined by XRD. The molecular structure of the unit of complex **I** and the crystal packing fragment of MOF **I** are shown in Figs. 1 and 2, respectively.

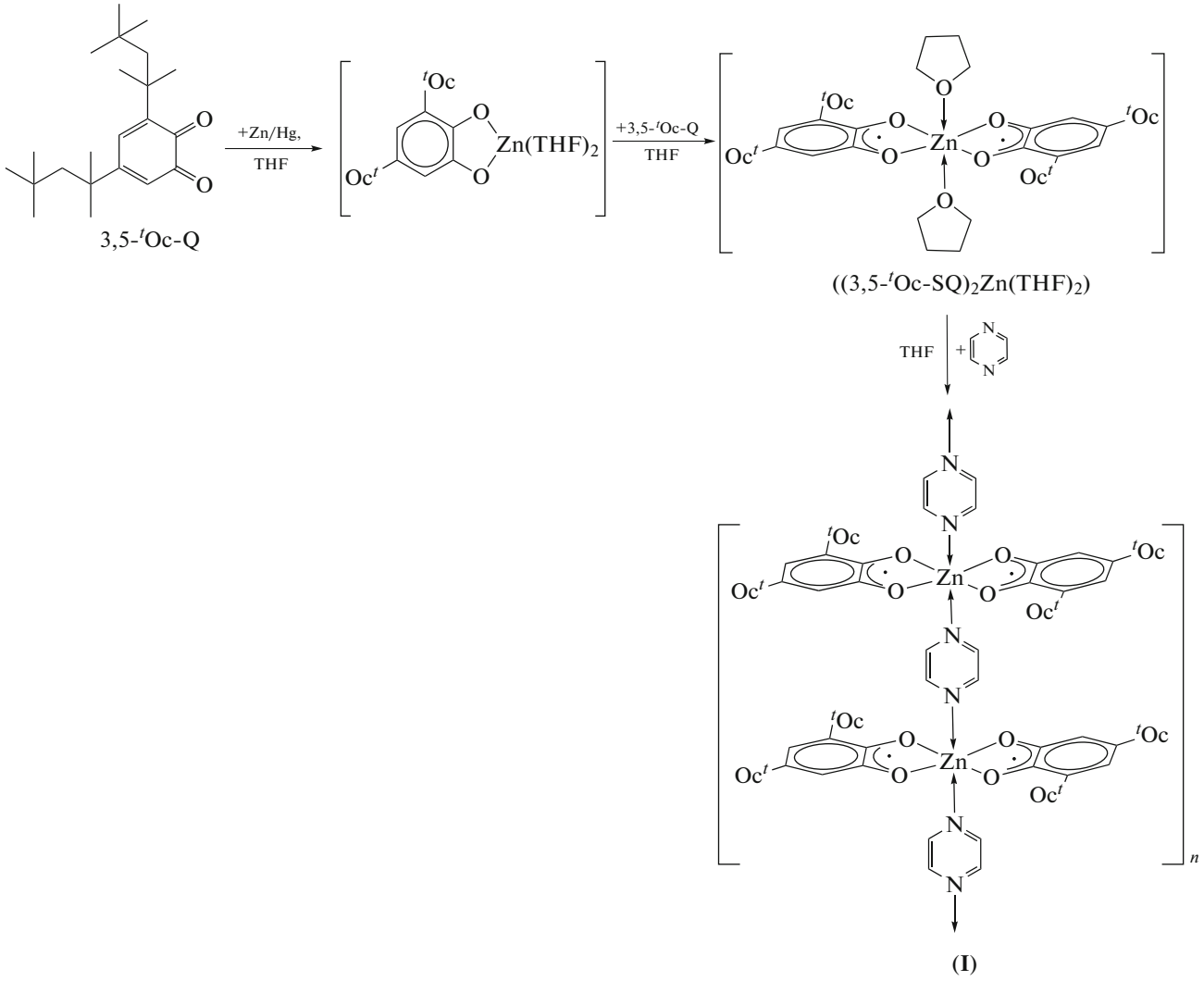

Scheme 1.

The molecular structure of complex **I** was determined by XRD. The coordination environment of the zinc atom in complex **I** is a distorted octahedron with the O(1), O(2), O(2A), and O(1A) atoms in the equatorial plane and the N(1) and N(2) atoms at the vertices (Fig. 3). The N(1)Zn(1)N(2) angle is 180.0, and the O(1)Zn(1)O(1A) and O(2)Zn(1)O(2A) angles are 178.14(6)° and 172.31(6)°, respectively. The planes of the diolate ligands deviate toward one of two pyrazine molecules due to which the Zn(1)–N(1) and Zn(1)–N(2) bond lengths are inequivalent being 2.234(2) and 2.396(2) Å, respectively. The C(1,2)-O(1,2) bond lengths are 1.2850(18) and 1.2791(19) Å and are characteristic of the sesquilateral C–O bonds in the *o*-semiquinolate metal complexes [51, 53, 58, 66]. The Zn(1)–O(1,2) bond lengths (2.0271(11) and 2.0425(11) Å, respectively) lie in the range of values typical of zinc *o*-semiquinolates [52, 67]. The diolate ligand exhibits quinoid alternation characteristic of the anion-radical form of the *o*-quinone ligand [68]. The polymer chains in complex **I** are parallel to each other (Fig. 2). Short π,π contacts, which are rather abundant in similar systems [51, 53], are not observed between the aromatic fragments in complex **I**. As

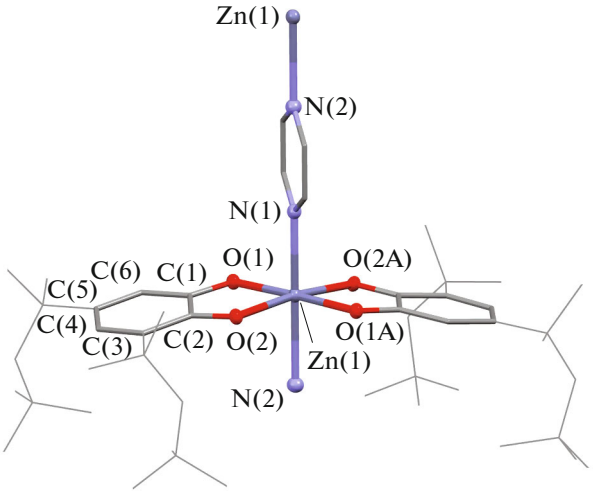

Fig. 1. Molecular structure of the unit of MOF **I**. Thermal ellipsoids of 30% probability are given for the key atoms. Hydrogen atoms are omitted for clarity.

expected, this is associated with the long and bulky *tert*-octyl substituents in the *o*-quinone ligands. Remarkably, all the four *tert*-octyl substituents are arranged at one side from the plane of the *o*-semiquinone ligands maximally efficiently shielding the SQ_2Zn fragments from each other in the framework of one polymer chain.

The exchange reaction of sodium 3,5-di-^{t}Oc-*o*-semiquinolate [59] and zinc diiodide (Scheme 2) was conducted as an attempt to prepare the same polymer product by the counter synthesis. However, the expected precipitation of sodium iodide from the reaction mixture does not occur even after the repeated dissolution of the obtained product in toluene. The addition of a pyrazine solution in toluene to the resulting mixture followed by the replacement of the solvent by hexane led to the formation of crystalline tetranuclear cluster complex **II**, which includes, according to the XRD data, the double contents of the following fragments: zinc bis-*o*-semiquinolate, sodium iodide, THF molecule, and pyrazine coordinated via the monodentate mode. The molecular and crystal structures of complex **II** were determined by XRD. The molecular structure of complex **II** is shown in Fig. 3. Selected bond lengths and angles in complex **II** are listed in Table 2. It is noteworthy that the unexpected involvement of sodium iodide in the formation of the polynuclear complex in the synthesis of the *o*-quinone metal derivatives is observed for the first time and is related, most likely, to the presence of the branched *tert*-octyl substituents that shield, to a high extent, the internal sphere of the polynuclear complex thus inducing the solubilization effect for NaI.

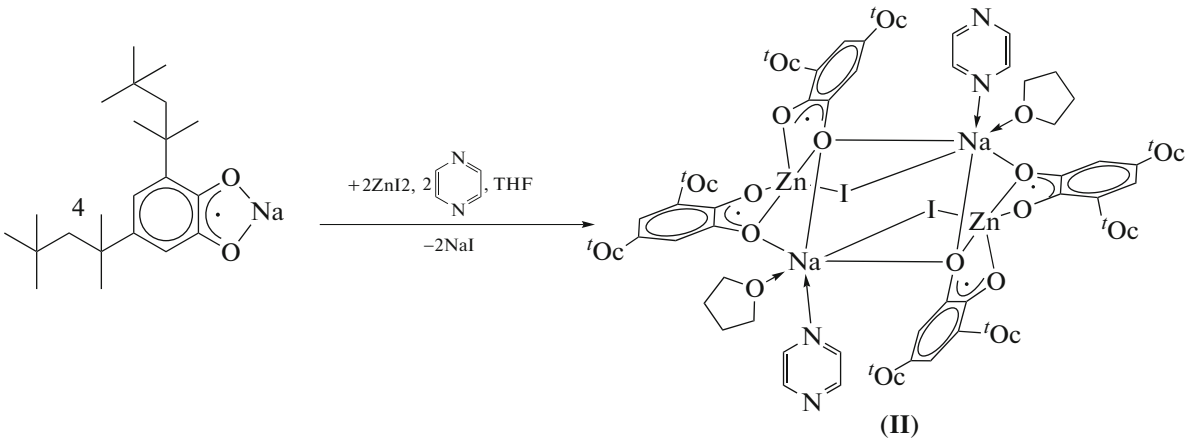

Scheme 2.

The zinc atom in complex **II** has a distorted square pyramidal environment (Fig. 4). The O(1), O(2), O(3), and O(4) atoms lie in the base of the pyramid, and the I(1) atom occupies the axial vertex. Zinc is elevated above the plane of the pyramid base by 0.676 Å. The Zn(1)–I(1) distance is less than the sum of the van der Waals radii of the elements (2.74 Å) [69, 70] and is equal to 2.5836(6) Å, which indicates the coordination interaction between the zinc and iodine atoms. Unlike polymer product **I**, polynuclear complex **II** exhibits a different mutual arrangement of the *tert*-octyl substituents: three of four branched alkyl substituents are directed toward the opposite side from the vertex of the tetragonal pyramid, and one substituent is directed toward Zn–I bond. The C(1,2,7,8)-O(1,2,3,4) bond lengths range from 1.262(5) to 1.277(5) Å and are characteristic of the sesquilateral C–O bonds in the metal *o*-semiquinolate complexes [51, 55]. The Zn(1)–O(1,2,3,4) bond lengths (2.015(3)–2.082(3) Å) lie in the range of values typical of the zinc *o*-semiquinolate complexes [52, 67]. The diolate ligand exhibits quinoid alternation characteristic of the *o*-semiquinolate ligands [68].

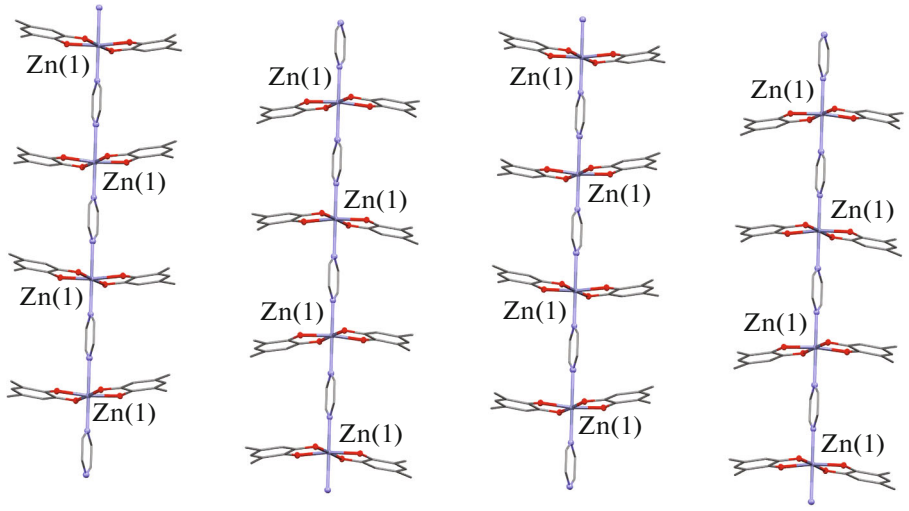

Fig. 2. Fragment of the crystal packing of MOF **I**. Thermal ellipsoids of 30% probability are given for the key atoms. *tert*-Octyl substituents are presented by the first quaternary carbon atom, and hydrogen atoms are omitted for clarity.

The environment of the sodium atom in polynuclear complex **II** is a distorted octahedron with the N(1), O(5), O(4A), and O(4) atoms in the plane and the I(1A) and O(2) atoms at the vertices (Fig. 5). The I(1A)Na(1)O(2) angle is 174.27(10)°. The Na(1)–I(1A) distance corresponds to the covalent binding between the elements (the sum of covalent radii of sodium and iodine is 3.21 Å [69]) and is equal to 3.1960(15) Å, which is a statistical average of the bond lengths between the aforementioned elements in the known complexes [71–78].

The EPR spectrum of polymer **I** in both the crystalline state and a toluene solution represents a broad unresolved singlet at room temperature and in the vitrified matrix of the solvent. This indicates that the oligomeric structure of the compound is retained in the solution and the polymer chain is not completely divided into monomeric pentacoordinate fragments. The EPR spectrum of complex **II** in the vitrified toluene matrix demonstrates a superposition of several signals characteristic of biradical particles (Fig. 6). A similar spectrum was observed [79] for related zinc

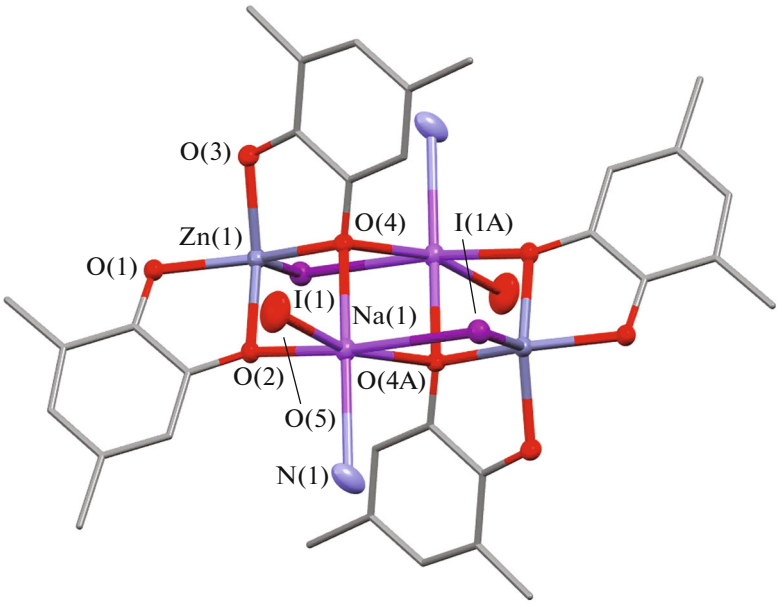

Fig. 3. Molecular structure of complex **II**. Thermal ellipsoids of 30% probability are given for the key atoms. *tert*-Octyl substituents are presented by the first quaternary carbon atom, pyrazines are presented by the coordinated nitrogen atom, and hydrogen atoms are omitted for clarity.

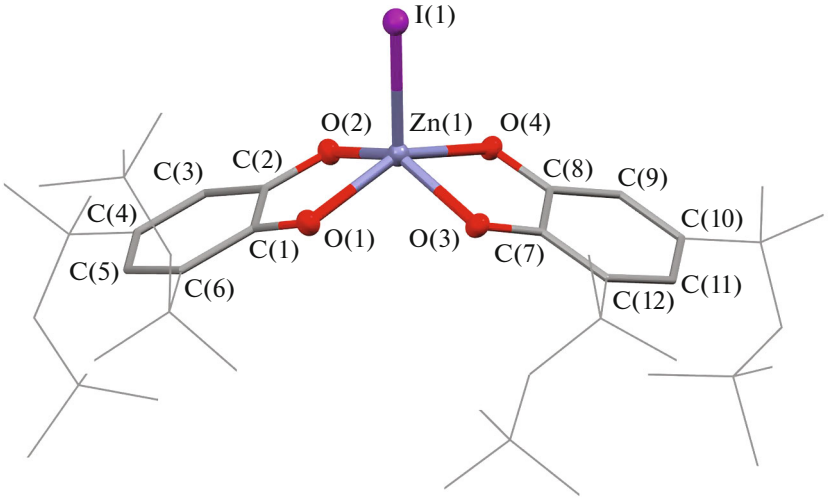

Fig. 4. Fragment of complex **II** (coordination environment of the Zn(1) atom).

bis-3,5-di-*tert*-butyl-*o*-semiquinolate. The superposition of numerous signals in the EPR spectrum of complex **II** can be explained by its polynuclear organization. The molecular structure of compound **II** assumes a possibility of three different dipole–dipole interactions between the radical centers: the first interaction occurs between the *o*-semiquinone ligands coordinated on one metal, and two interactions take place between unpaired electrons of the *o*-semiquinolate ligands bound to different zinc atoms. In addition, intermolecular contacts due to hydrogen bonds involving the uncoordinated nitrogen atom of pyrazine should not be excluded.

The experimental dependences $\mu_{eff}(T)$ for the crystalline samples of complexes **I** and **II** are shown in Fig. 7. For complex **I** at 300 K, μ_{eff} = 2.48 μ_B and is well consistent with a theoretical spin-only value of 2.45 μ_B for two paramagnetic centers with the spins $S = 1/2$. With decreasing temperature μ_{eff} decreases first gradually and below 70 K more sharply reaching 0.84 μ_B at 5 K. A decrease in μ_{eff} with decreasing temperature indicates the predomination of exchange interactions of the antiferromagnetic character. The model of exchange-bonded dimer ($H = -2JS_1S_2$) unsatisfactorily describes the experimental data (Fig. 7a, red curve). It is most likely that antiferromagnetic interactions occur not only in the (3,5-^{t}Oc-SQ)$_2$Zn bis(chelate) fragments but also between them in the polymer chains via the π orbitals of the bridging pyrazine molecules. The sensitivity of the exchange interactions between spins of the *o*-semiquinolate ligands to the electronic structures of the additional ligand has been shown previously [80, 81]. The theoretical curve taking into account both the exchange interactions J_1 in the (3,5-^{t}Oc-SQ)$_2$Zn bis(chelate) fragments and the J_2 interactions between them describes well the experimental data (Fig. 7a, green curve). The optimum values of parameters J_1 and J_2 obtained by an analysis of the $\mu_{eff}(T)$ dependence are -9.8 ± 0.1 and -8.4 ± 0.1 cm^{-1}, respectively.

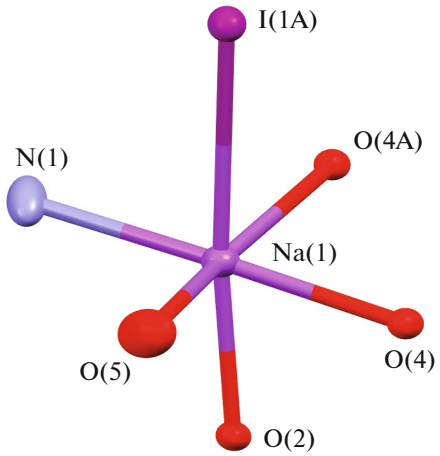

Fig. 5. Fragment of complex **II** (coordination environment of the Na(1) atom).

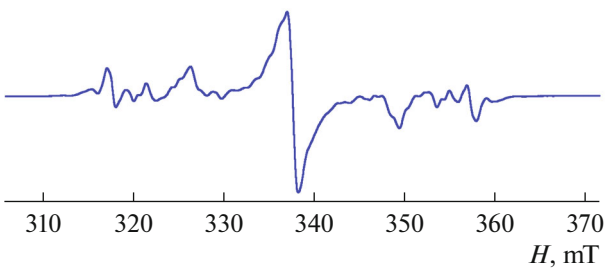

Fig. 6. EPR spectrum of complex **II** in the frozen matrix of the solvent (toluene–CH_2Cl_2, 150 K).

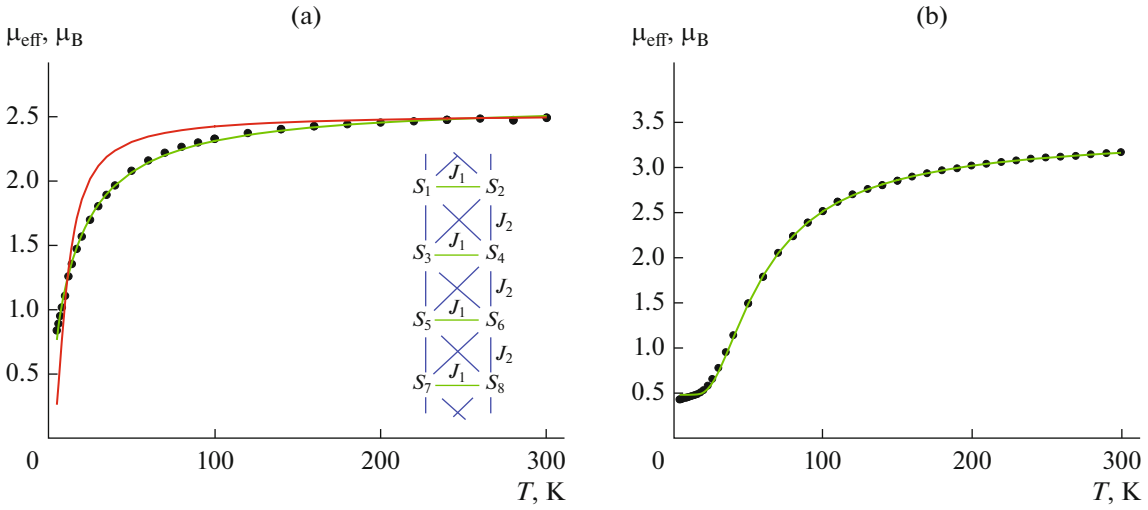

Fig. 7. Dependences $\mu_{eff}(T)$ for (a) **I** and (b) **II**. Solid lines are theoretical curves.

For complex **II** at 300 K, $\mu_{eff} = 3.17\ \mu_B$, which is slightly lower than the theoretical spin-only value (3.46 μ_B) for four paramagnetic centers with the spins $S = 1/2$. With decreasing temperature, μ_{eff} decreases first gradually and below 150 K more sharply reaching a plateau of ~0.45 μ_B below 15 K. In the case of complex **II**, the $\mu_{eff}(T)$ dependence is well described by the model assuming only exchange interactions J in the (3,5-^{t}Oc-SQ)$_2$Zn bis(chelate) fragments with allowance for monomer impurity p, which causes the nonzero value of μ_{eff} at low temperatures. For an analysis of the experimental data using the four-spin exchange cluster model (spin-Hamiltonian $H = -2J(S_1S_2 + S_3S_4)$, the optimum values of parameters J and p are -52.0 ± 0.1 cm^{-1} and $p = 1.9\%$, respectively. Taking into account additional exchange interactions between spins of *o*-semiquinones of the adjacent bis(chelate) fragments in the molecule of complex **II** exerts almost no effect on the value of parameter J but results in transparametrization. Note that the exchange parameters in the octahedral (**I**) and square pyramidal (**II**) complexes turned out to be close to those for the already known zinc compounds with a similar environment of the metallocenter, respectively [51, 52, 55].

As assumed, the introduction of the sterically hindered substituent, such as the *tert*-octyl fragment, into the organic ligand affected the fact that the magnetic properties of the synthesized compounds began to be determined, to a high extent, by the intramolecular exchange interactions. As a result, interchain or intermolecular exchange interactions can be ignored when analyzing the $\mu_{eff}(T)$ dependences for complexes **I** and **II**. The significant differences in the magnetic behavior of the complexes are due to specific features of the arrangement of the paramagnetic ligands in the coordination nodes. For instance, a decrease in the angle between the *o*-semiquinolate planes in the (3,5-^{t}Oc-SQ)$_2$Zn bis(chelate) fragments leads to an increase in the energy of exchange interactions, and the cluster form with the square pyramidal environment of the metal demonstrates much stronger antiferromagnetic exchanges than the polymer form with the octahedral environment of the metallocenter. It is interesting that different synthetic approaches to the synthesis of the compounds make it possible to prepare complexes of different types: polymer chains or polynuclear clusters.

ACKNOWLEDGMENTS

This work was carried out using the equipment of the Center for Collective Use "Analytical Center of Institute of Organometallic Chemistry of Russian Academy of Sciences" and supported by the project "Provision of Development of Material Technical Infrastructure of Centers for Collective Use of Scientific Equipment" (unique identifier RF–2296.61321X0017, agreement no. 075-15-2021-670). The XRD studies of complexes **I** and **II** were conducted using the equipment of the Center for Collective Use of Physical Methods of Investigation at the Kurnakov Institute of General and Inorganic Chemistry (Russian Academy of Sciences).

FUNDING

This work was supported by the Council on Grants of the President of the Russian Federation aimed at supporting leading scientific schools, project no. NSh-403.2022.1.3.

CONFLICT OF INTEREST

The author of this work declares that they has no conflicts of interest.

REFERENCES

1. Pierpont, C.G., *Coord. Chem. Rev.*, 2001, vols. 219–221.
2. Ershova, I.V., Piskunov, A.V., and Cherkasov, V.K., *Russ. Chem. Rev.*, 2020, vol. 89, p. 1157. https://doi.org/10.1070/RCR4957
3. Bubnov, M.P., Piskunov, A.V., Zolotukhin, A.A., et al., *Russ. J. Coord. Chem.*, 2020, vol. 46, p. 224. https://doi.org/10.31857/S0132344X20030019
4. Kaim, W., Das, A., Fiedler, J., et al., *Coord. Chem. Rev.*, 2020, vol. 404, p. e213114.
5. Rajput, A., Sharma, A.K., Barman, S.K.A., et al., *Coord. Chem. Rev.*, 2020, vol. 414, p. e213240.
6. Pashanova, K.I., Poddel'sky, A.I., and Piskunov, A.V., *Coord. Chem. Rev.*, 2022, vol. 459, p. 214399.
7. Chegerev, M.G. and Piskunov, A.V., *Russ. J. Coord. Chem.*, 2018, vol. 44, p. 258. https://doi.org/10.7868/S0132344X18020044
8. Ershova, I.V. and Piskunov, A.V., *Russ. J. Coord. Chem*, 2020, vol. 46, no. 3, p. 154. https://doi.org/10.31857/S0132344X20030020
9. Pierpont, C.G., *Coord. Chem. Rev.*, 2001, vols. 216–217, p. 99.
10. Buchanan, R.M. and Pierpont, C.G., *J. Am. Chem. Soc.*, 1980, vol. 102, p. 4951.
11. Shapovalova, S.O., Guda, A.A., Bubnov, M.P., et al., *Chem. Lett.*, 2021, vol. 50, p. 1933.
12. Bubnov, M.P., Skorodumova, N.A., Fukin, G.K., et al., *Polyhedron*, 2021, vol. 209, p. 115485.
13. Tezgerevska, T., Alley, K.G., and Boskovic, C., *Coord. Chem. Rev.*, 2014, vol. 268, p. 23.
14. Drath, O., Gable, R.W., Moubaraki, B., et al., *Inorg. Chem.*, 2016, vol. 55, p. 4141.
15. Hendrickson, D.N. and Pierpont, C.G., *Top. Curr. Chem.*, 2004, vol. 234, p. 63.
16. Jung, O.-S. and Pierpont, C.G., *J. Am. Chem. Soc.*, 1994, vol. 116, p. 2229.
17. Bubnov, M.P., Kozhanov, K.A., Skorodumova, N.A., et al., *Inorg. Chem.*, 2020, vol. 59, p. 6679.
18. Zolotukhin, A.A., Bubnov, M.P., Arapova, A.V., et al., *Inorg. Chem.*, 2017, vol. 56, p. 14751.
19. Guda, A.A., Chegerev, M.G., Starikov, A.G., et al., *J. Phys.: Condens. Matter*, 2021, vol. 33, p. 215405.
20. Ilyakina, E.V., Poddel'sky, A.I., Cherkasov, V.K., et al., *Mendeleev Commun.*, 2012, vol. 22, p. 208.
21. Cherkasov, V.K., Abakumov, G.A., Grunova, E.V., et al., *Chem.-Eur. J.*, 2006, vol. 12, p. 3916.
22. Arsenyeva, K.V., Klimashevskaya, A.V., Pashanova, K.I., et al., *Appl. Organomet. Chem.*, 2022, vol. 36, no. 4., p. e6593.
23. Ershova, I.V., Meshcheryakova, I.N., Trofimova, O.Y., et al., *Inorg. Chem.*, 2021, vol. 60, p. 12309.
24. Ershova, I.V., Meshcheryakova, I.N., Trofimova, O.Y., et al., *Inorg. Chim. Acta*, 2022, vol. 535, p. 121031.
25. Pashanova, K.I., Bitkina, V.O., Yakushev, I.A., et al., *Molecules*, 2021, vol. 26, p. 4622.
26. Maleeva, A.V., Ershova, I.V., Trofimova, O.Y., et al., *Mendeleev Commun.*, 2022, vol. 32, p. 83.
27. Ershova, I.V., Maleeva, A.V., Aysin, R.R., et al., *Russ. Chem. Bull.*, 2023, vol. 72, no. 1, p. 193. https://doi.org/10.1007/s11172-023-3724-2
28. Maleeva, A.V., Trofimova, O.Y., Ershova, I.V., et al., *Russ. Chem. Bull.*, 2022, vol. 71, p. 1441. https://doi.org/10.1007/s11172-022-3550-y
29. Cameron, L.A., Ziller, J.W., and Heyduk, A.F., *Chem. Sci.*, 2016, vol. 7, p. 1807.
30. Kramer, W.W., Cameron, L.A., Zarkesh, R.A., et al., *Inorg. Chem.*, 2014, vol. 53, p. 8825.
31. Archer, S. and Weinstein, J.A., *Coord. Chem. Rev.*, 2012, vol. 256, p. 2530.
32. BaniKhaled, M.O., Becker, J.D. Koppang, M., et al., *Cryst. Growth Des.*, 2016, vol. 16, p. 1869.
33. Tichnell, C.R., Daley, D.R., Stein, B.W., et al., *J. Am. Chem. Soc.*, 2019, vol. 141, p. 3986.
34. Stein, B.W., Tichnell, C.R., Chen, J., et al., *J. Am. Chem. Soc.*, 2018, vol. 140, p. 2221.
35. Kirk, M.L., Shultz, D.A., Chen, J., et al., *J. Am. Chem. Soc.*, 2021, vol. 143, p. 10519.
36. Kirk, M.L., Shultz, D.A., Hewitt, P., et al., *Chem. Sci.*, 2021, vol. 12, p. 13704.
37. Kirk, M.L., Shultz, D.A., Hewitt, P., et al., *J. Am. Chem. Soc.*, 2022, vol. 144, p. 12781.
38. Shavaleev, N.M., Davies, E.S., Adams, H., et al., *Inorg. Chem.*, 2008, vol. 47, p. 1532.
39. Yang, J., Kersi, D., Giles, L.J., et al., *Inorg. Chem.*, 2014, vol. 53, p. 4791.
40. Sobottka, S., Noßler, M., Ostericher, A.L., et al., *Chem.-Eur. J.*, 2020, vol. 26, p. 1314.
41. Ovcharenko, V.I. and Sagdeev, R.Z., *Russ. Chem. Rev.*, 1999, vol. 68, p. 345.
42. Koivisto, B.D. and Hicks, R.G., *Coord. Chem. Rev.*, 2005, vol. 249, p. 2612.
43. Ratera, I. and Veciana, J., *Chem. Soc. Rev.*, 2012, vol. 41, p. 303.
44. Iwamura, H., *Polyhedron*, 2013, vol. 66, p. 3.
45. Faust, T.B. and D'Alessandro, D.M., *RSC Adv.*, 2014, vol. 4, p. 17498.
46. Vostrikova, K.E., *Coord. Chem. Rev.*, 2008, vol. 252, nos. 12–14, p. 1409.
47. Halcrow, M.A., *Spin-Crossover Materials. Properties and Applications*, New York: Wiley, 2013.
48. Poddel'sky, A.I., Cherkasov, V.K., and Abakumov, G.A., *Coord. Chem. Rev.*, 2009, vol. 253, p. 291.
49. Paretzki, A., Hubner, R., Ye, S., et al., *Mater. Chem. C*, 2015, vol. 3, p. 4801.
50. Paretzki, A., Bubrin, M., Fiedler, J., et al., *Chem.-Eur. J.*, 2014, vol. 20, p. 5414.
51. Piskunov, A.V., Maleeva, A.V., Bogomyakov, A.S., et al., *Polyhedron*, 2015, vol. 102, p. 715.
52. Piskunov, A.V., Maleeva, A.V., Fukin, G.K., et al., *Inorg. Chim. Acta*, 2017, vol. 455, p. 213.
53. Piskunov, A.V., Maleeva, A.V., Bogomyakov, A.S., et al., *Russ. Chem. Bull.*, 2017, vol. 66, p. 1618.
54. Bellan, E.V., Poddel'sky, A.I., Protasenko, N.A., et al., *Inorg. Chem. Commun.*, 2014, vol. 50, p. 1.

55. Piskunov, A.V., Maleeva, A.V., Bogomyakov, A.S., et al., *Russ. J. Coord. Chem.*, 2019, vol. 45, p. 309. https://doi.org/10.1134/S0132344X19050025
56. Perrin, D.D., Armarego, W.L.F., and Perrin, D.R., *Purification of Laboratory Chemicals*, Oxford: Perrin Pergamon, 1980.
57. Kocherova, T.N., Druzhkov, N.O., Arsenyev, M.V., et al., *Russ. Chem. Bull.*, 2023, vol. 72, no. 5, p. 1192.
58. Piskunov, A.V., Maleeva, A.V., Abakumov, G.A., et al., *Russ. J. Coord. Chem.*, 2011, vol. 37, p. 243. https://doi.org/10.1134/S1070328411030092
59. Piskunov, A.V., Mescheryakova, I.N., Bogomyakov, A.S., et al., *Inorg. Chem. Commun.*, 2009, vol. 12, p. 1067.
60. *Bruker, APEX3, SAINT, and, SADABS*, Madison: Bruker, AXS, Inc., 2016.
61. Krause, L., Herbst-Irmer, R., Sheldrick, G.M., and Stalke, D., *J. Appl. Crystallogr.*, 2015, vol. 48, p. 3.
62. Sheldrick, G.M., *Acta Crystallogr., Sect. A: Found. Adv.*, 2015, vol. 71, p. 3.
63. Sheldrick, G.M., *Acta Crystallogr. Sect. C: Struct. Chem.*, 2015, vol. 71, p. 3.
64. Spek, A.L., *Acta Crystallogr. Sect. C: Struct. Chem.*, 2015, vol. 71, p. 9.
65. Dolomanov, O.V., Bourhis, L.J., Gildea, R.J., et al., *J. Appl. Crystallogr.*, 2009, vol. 42, p. 339.
66. Brown, S.N., *Inorg. Chem.*, 2012, vol. 51, p. 1251.
67. Glavinović, M., Qi, F., Katsenis, A.D., et al., *Chem. Sci.*, 2016, vol. 7, p. 707.
68. Piskunov, A.V., Meshcheryakova, I.N., Maleeva, A.V., et al., *Eur. J. Inorg. Chem.*, 2014, no. 20, p. 3252.
69. Batsanov, S.S., *Russ. J. Inorg. Chem.*, 1991, vol. 36, no. 12, p. 1694.
70. Emsley, J., *Elements*, Oxford: Clarendon, 1991.
71. Dankert, F. and Hanisch, C., *Inorg. Chem.*, 2019, vol. 58, p. 3518.
72. Sugimoto, K., Takaya, H., Maekawa, M., et al., *Cryst. Growth Des.*, 2018, vol. 18, p. 571.
73. Dange, D., Choong, S.L., Schenk, C., et al., *Dalton Trans.*, 2012, vol. 41, p. 9304.
74. Li, F., Yin, H., and Wang, D., *Acta Crystallogr., Sect. E: Struct. Rep. Online*, 2006, vol. 62, p. m437.
75. Zábranský, M., Císarováa, I., and Stěpnička, P., *Dalton Trans.*, 2015, vol. 44, p. e14494.
76. Raston, C.L., Whitaker, C.R., and White, A.H., *Aust. J. Chem.*, 1989, vol. 42, p. 1393.
77. Voegel, J.C., Thierry, J.C., and Weiss, R., *Acta Crystallogr., Sect. B: Struct. Sci.*, 1974, vol. 30, p. 56.
78. Knölker, H.-J., Baum, E., Goesmann, H., et al., *Angew. Chem., Int. Ed. Engl.*, 1999, vol. 38, p. 2064.
79. Ozarowski, A., McGarvey, B.R., Peppe, C., et al., *J. Am. Chem. Soc.*, 1991, vol. 113, p. 3288.
80. Ovcharenko, V.I., Gorelik, E.V., Fokin, S.V., et al., *J. Am. Chem. Soc.*, 2007, vol. 129, p. 10512.
81. Piskunov, A.V., Ershova, I.V., Bogomyakov, A.S., et al., *Inorg. Chem.*, 2015, vol. 54, p. 6090.

Translated by E. Yablonskaya